HHS Public Access

Author manuscript

Eur Radiol. Author manuscript; available in PMC 2017 August 18.

Published in final edited form as:

Eur Radiol. 2017 January ; 27(1): 32–40. doi:10.1007/s00330-016-4375-6.

Combined gadoxetic acid and gadofosveset enhanced liver MRI for detection and characterization of liver metastases

Peter Bannas[1,2], **Candice A. Bookwalter**[1], **Tim Ziemlewicz**[1], **Utaroh Motosugi**[1,3], **Alejandro Munoz del Rio**[1], **Theodora A. Potretzke**[1], **Scott K. Nagle**[1,4,5], and **Scott B. Reeder**[1,4,6,7,8]

[1]Department of Radiology, University of Wisconsin-Madison, Madison, WI, USA

[2]Department of Radiology, University Hospital, University Medical Center Hamburg-Eppendorf, Martinistrasse 52, 20246 Hamburg, Germany

[3]Department of Radiology, University of Yamanashi, Yamanashi, Japan

[4]Department of Medical Physics, University of Wisconsin-Madison, Madison, WI, USA

[5]Department of Pediatrics, University of Wisconsin-Madison, Madison, WI, USA

[6]Department of Biomedical Engineering, University of Wisconsin-Madison, Madison, WI, USA

[7]Department of Medicine, University of Wisconsin-Madison, Madison, WI, USA

[8]Department of Emergency Medicine, University of Wisconsin-Madison, Madison, WI, USA

Abstract

Purpose—To compare gadoxetic acid alone and combined gadoxetic acid/gadofosveset trisodium-enhanced liver MRI for detection of metastases and differentiation of metastases from haemangiomas.

Methods—Ninety-one patients underwent gadoxetic acid-enhanced liver MRI before and after additional injection of gadofosveset. First, two readers retrospectively identified metastases on gadoxetic acid alone enhanced delayed hepatobiliary phase T1-weighted images together with all other MR images (dynamic images, T2-weighted images, diffusion-weighted images). Second, readers assessed additional T1-weighted images obtained after administration of gadofosveset trisodium. For both interpretations, readers rated lesion conspicuity and confidence in differentiating metastases from haemangiomas. Results were compared using alternative free-response receiver-operating characteristic (AFROC) and conventional ROC methods. Histology and follow-up served as reference standard.

Results—There were 145 metastases and 16 haemangiomas. Both readers detected more metastases using combined gadoxetic acid/gadofosveset (reader 1 =130; reader 2=124) compared to gadoxetic acid alone (reader 1 = 104; reader 2=103). Sensitivity of combined gadoxetic acid/gadofosveset (reader 1 = 90 %; reader 2 = 86 %) was higher than that of gadoxetic acid alone (reader 1=72 %; reader 2 = 71 %, both $P<0.01$). AFROC-AUC was higher for the combined

Correspondence to: Peter Bannas.

Electronic supplementary material The online version of this article (doi:10.1007/s00330-016-4375-6) contains supplementary material, which is available to authorized users.

technique (0.92 vs. 0.86, $P< 0.001$). Sensitivity for correct differentiation of metastases from haemangiomas was higher for the combined technique (reader 1 =98 %; reader 2 = 99 % vs. reader 1 = 86 %; reader 2 = 91 %, both $P<0.01$). ROC-AUC was significantly higher for the combined technique (reader 1 =1.00; reader 2=1.00 vs. reader 1 =0.87; reader 2=0.92, both $P<0.01$).

Conclusion—Combined gadoxetic acid/gadofosveset-enhanced MRI improves detection and characterization of liver metastases compared to gadoxetic acid alone.

Keywords

Magnetic resonance imaging; Liver; Metastases; Gadoxetic acid; Gadofosveset trisodium

Introduction

Metastatic disease to the liver dramatically impacts patient prognosis and mortality [1]. Accurate detection of the number and location of liver metastases is particularly important for patients whose metastatic burden is potentially curable by resection [2]. Multiple studies have demonstrated high diagnostic accuracy of magnetic resonance imaging (MRI) for detection of liver metastases [3,4].

Liver-specific contrast MRI contrast agents such as gadoxetic acid (Eovist, Primovist, Bayer Pharmaceuticals) can further improve the sensitivity for detection of liver metastases using delayed hepatobiliary phase T1-weighted MRI [5–7]. However, even with gadoxetic acid, not all metastases are detected and the sensitivity varies from 85 % to 95 % [5–8]. This is particularly true for small lesions (less than 1 cm) that are missed more often [7, 8]. Further, even if a small lesion is identified, a well-known challenge for hepatobiliary phase gadoxetic acid-enhanced MRI is the differentiation of small metastases from small cavernous haemangiomas [9–11]. In the hepatobiliary phase, both haemangiomas and metastases appear dark, similar to blood vessels, since enhancement of haemangiomas follows the blood pool [4, 12–14]. Diagnosis of large cavernous haemangiomas is generally straightforward and can be made through the combination of T2-weighted imaging, pre-contrast and dynamic post-contrast T1-weighted imaging and diffusion-weighted imaging. However, the enhancement pattern of small haemangiomas may be challenging to characterize and large cavernous haemangiomas may display atypical features, making the diagnosis uncertain [15, 16]. Given the high prevalence of haemangiomas, the ability to diagnose them with confidence is an important component of metastatic staging in the liver [10, 11, 17].

Gadofosveset trisodium (Ablavar, Lantheus Medical Imaging) is a gadolinium-based intravascular contrast agent with transient binding to serum albumin, which results in a steady-state blood pool of approx. 1 h [18]. A recent study used gadofosveset in an off-label fashion for the characterization of liver lesions and indicated that cavernous haemangiomas in the liver accumulate gadofosveset on delayed phase imaging while metastases do not [19]. The feasibility of combined gadoxetic acid and gadofosveset-enhanced off-label use for liver MRI in healthy volunteers has also been demonstrated [20]. The resulting images

demonstrated a homogenously hyperintense-appearing liver due to the gadoxetic acid-enhanced hepatocytes and bile and enhancement of blood vessels from gadofosveset [20].

We hypothesized that administration of gadofosveset during the hepatobiliary phase of gadoxetic acid would improve detection of metastases *and* differentiation of metastases from haemangiomas. Therefore, the purpose of this work was to compare the diagnostic accuracy of a gadoxetic acid alone and a combined gadoxetic acid/gadofosveset-enhanced liver MRI for detection and characterization of metastases.

Materials and methods

Patients

This Health Insurance Portability and Accountability Act (HIPAA)-compliant retrospective study was approved by our institutional review board. We identified 121 consecutive adults from our database who underwent combined gadoxetic acid and gadofosveset liver MRI for diagnosis, detection and/or staging of liver metastasis as per standard clinical protocol between January 2014 and October 2014. We note that the use of gadofosveset for detection and characterization of focal liver lesions is an off-label use of this agent.

A radiologist (P.B.) with 8 years of experience in abdominal radiology retrospectively determined the patients' eligibility for this study. A total of 91 patients (48 men, 43 women; mean age 58.1 ± 13.1 years) were included if they met at least one of the following criteria (Fig. 1): (i) patients with histologically proven liver metastases (n = 18); (ii) patients with histologically proven primary malignancy and with liver metastases that were proven by definite increase or decrease in size by follow-up imaging of 3–6months (n =13); (iii) patients with haemangiomas that had typical imaging features on dynamic contrast-enhanced CT [21] or abdominal ultrasonography [22] within 1 month and stable size for more than 6 months on previous or follow-up imaging [22, 23](n=12); (iv) patients without metastases or haemangiomas, confirmed by either abdominal ultrasound or dynamic CT performed more than 3 months after MRI (n = 48). Patients who did not match any of the above criteria (n = 21) or with more than 10 liver metastases (too many to analyse) (n =9) were excluded.

Reference standard

Two board-certified radiologists (P.B. and U.M. with 8 and 14 years of experience, respectively) reviewed together and by consensus all gadoxetic acid alone and all combined gadoxetic acid/gadofosveset images to identify all focal liver lesions. All other sequences, viz. dynamic imaging, T2-weighted imaging (T2WI) and diffusion-weighted imaging (DWI), were available for review. The readers had access to all other prior and follow-up imaging examinations (MRI, CT, ultrasound, PET/CT), as well as histopathological and clinical results to establish the ground truth reading. The readers detected a total of 145 metastases in the 31 patients with malignancy. The mean number of metastases per patient was 4 7 (range 1–10) Metastases were confirmed by either histology (criteria (i), n = 47) or follow-up imaging (criteria (ii), n = 98, increase in size, n = 71; decrease in size after treatment, n = 27). Sixteen haemangiomas were found in 12 patients, which were confirmed

by either dynamic CT (n = 10) or ultrasonography with follow-up examination (n = 6). None of the patients with metastases had any haemangiomas.

In the 31 patients with metastatic disease, the primary malignancies were as follows: colonic adenocarcinoma (n =14), carcinoid (n = 5), melanoma (n = 3), pancreatic adenocarcinoma (n = 3), oesophageal adenocarcinoma (n = 2), biliary adenocarcinoma (n = 1), renal cell carcinoma (n = 1), endometrial cancer (n = 1) and lung cancer (n = 1). Twenty-one of the patients (67.7 %) had been treated with intravenous chemotherapy.

MR imaging and injection protocol

Imaging was performed on either 1.5-T or 3-T MR systems (GE Healthcare, Waukesha, WI) using an eight-channel and 32-channel phased-array body receive-only coil, respectively. The routine MR imaging protocol for 20-min hepatobiliary phase imaging with gadoxetic acid was performed with two additional imaging sequences after additional injection of gadofosveset trisodium as detailed in Fig. 2.

The imaging protocol included axial fat-saturated breathheld T2WI, DWI, and unenhanced and dynamic enhanced T1-weighted gradient-echo imaging (T1WI).

At 1.5 T the imaging parameters included (1) T2WI: TR/TE 1286/98 ms, field-of-view (FOV) 32×29 cm, matrix 320×224, slice thickness 5 mm; (2) DWI: TR/TE 15,000/57 ms, FOV 36 × 36 cm, matrix 200 × 160, B values of 50 and 500; (3) T1WI: TR/TE 3.6/1.7 ms, flip angle 12°, FOV 38×27 cm, matrix 256 × 192, slice-thickness 5 mm. At 3 T the imaging parameters were (1) T2WI: TR/TE 15,000/88 ms, FOV 40 × 32 cm, matrix 320 × 224, slice thickness 5 mm, (2) DWI: TR/TE 13,333/61 ms, FOV 38×38 cm, matrix 192 × 192, B values of 50 and 500; (3) T1WI: TR/TE 4.2/1.9 ms, flip angle 15°, FOV 40×32 cm, matrix 288 × 192, slice thickness 3.6 mm for T1WI.

Dynamic T1WI acquisitions with 5-mm sections were performed at approx. 30 s (arterial phase was fluoro-triggered), 50 s, 2 min, 5 min and 20 min (hepatobiliary phase) after injection of 0.05 mmol/kg of gadoxetic acid (Eovist, Bayer Healthcare, Wayne, NJ) at 2 mL/s through a 20-G antecubital intravenous catheter followed by a 20-mL chaser of normal saline at the same injection rate. Immediately after the 20-min acquisition a respiratory-gated free-breathing T1WI gradient-echo sequence was performed with a higher flip angle of 30°. The free-breathing technique acquired images with thin sections of 1.8 mm (1.5 T) or 1.6 mm (3 T) with high signal-to-noise ratio [24, 25].

Subsequently, 0.05 mml/kg of gadofosveset trisodium was injected by hand. Both the breathheld low flip angle and the respiratory-gated high flip angle T1WI acquisitions were repeated 5 min after injection of gadofosveset.

Detection of metastases

Two radiologists (C.A.B. and T.Z. with 6 and 10 years of experience, respectively) performed individual reading of MR images in a randomized fashion, blinded to the results of other imaging studies and clinical diagnoses.

First, the readers were presented the gadoxetic acid alone enhanced images together with all other MR images (T2w, dynamic imaging, DWI) except the combined gadoxetic acid/gadofosveset images. The readers recorded the location of metastases (individual image number, segmental location and size) by marking the individual locations on schematic anatomical diagrams of the liver. Each mark was assigned with a confidence rating on a four-point scale: 1 = probably not a lesion/almost missed; 2 = possible lesion; 3 = probable lesion; 4 = definite lesion/stands out unmistakably [26].

Second, the readers were presented the additional T1WI images obtained after administration of gadofosveset trisodium, in addition to all other acquisitions. The readers recorded the presence, location and confidence for all previously detected metastases and any additional metastases detected on combined gadoxetic acid/gadofosveset-enhanced images. Readers were also instructed to indicate the presence and location of any haemangiomas.

Distinguishing metastasis from haemangioma

Reader 1 and reader 2 independently graded each lesion identified on both gadoxetic acid alone and combined gadoxetic acid/gadofosveset-enhanced images using a five-point scale to determine the diagnostic accuracy of the two techniques to differentiate metastasis from haemangioma: 1 = certainly haemangioma; 2 = likely haemangioma; 3 = indeterminate; 4 = likely metastasis; 5 = certainly metastasis [9]. Both gadoxetic acid alone and combined gadoxetic acid/gadofosveset-enhanced images were rated together with all other MR images. The readers categorized the enhancement pattern of each lesion on both gadoxetic acid alone and combined gadoxetic acid/gadofosveset-enhanced delayed images: no/negligible enhancement; central enhancement with peripheral washout; ring enhancement; heterogeneous enhancement; peripheral nodular enhancement; homogenous enhancement, reaching approximate isointensity relative to the gadoxetic acid-enhanced liver tissue [19]. On the combined gadoxetic acid/gadofosveset-enhanced images, lesions were classified as haemangiomas if they showed homogenous enhancement or peripheral nodular enhancement with gadofosveset. Lesions were rated as metastases if they showed no or minimal enhancement, central enhancement, ring enhancement or heterogeneous enhancement. Lesions were rated as cysts if they were bright on T2-weighted images and showed no enhancement with gadofosveset.

Quantitative characterization of metastases and haemangiomas

We compared the relative signal intensities (SI) of metastases with haemangiomas before and after injection of gadofosveset. First, one radiologist (blinded) measured the diameters of all metastases and haemangiomas using an electronic caliper. The mean size for metastases (n = 145) was 12 ±11 mm (median 7, range 3–62 mm), 94 of the 145 metastases (64.8 %) were 10 mm or smaller. The mean size for haemangiomas (n = 16) was 17 ±20 mm (median 9, range 3–85 mm), 9 of the 16 haemangiomas (56.3 %) were 10 mm or smaller. Second, regions of interest (ROIs) were drawn on metastases (n = 88 in 24 patients) and haemangiomas (n =15 in 11 patients) with a size of 5 mm or smaller on the 1.8 mm (1.5 T) or 1.6 mm (3 T) sections to minimize partial volume effects. In addition, ROIs were drawn on the liver parenchyma (approx. 4 cm^2) adjacent to each lesion.

Statistical analysis

The diagnostic performance of detecting liver metastases on gadoxetic alone and combined gadoxetic/gadofosveset-enhanced images was compared using alternative free-response ROC (AFROC) analysis [6, 26]. AFROC curves were calculated for each reader and the average of both readers. The performance of both techniques was evaluated by comparing the area under the curves (AUC) using an internal *F* test [27, 28]. The sensitivity and positive predictive value (PPV) were calculated using generalized estimating equations (GEE) [29] to account for data clustering (i.e. multiple lesions in a single patient). A log-binomial link was used, and the working correlation matrix was assumed to be independent; 95 % confidence intervals (CI) were based on robust sandwich variance estimators. Each marked lesion was used as a reader's judgment for a positive finding. Sensitivities were compared with a McNemar's test adjusted for clustering [30]; PPVs were compared with a Chi-squared test adjusted for clustering [31].

The discriminatory ability of combined gadoxetic acid/gadofosveset relative to gadoxetic acid alone to distinguish between haemangioma and metastasis was determined by comparing cluster-adjusted AUCs of conventional non-parametric ROC curves [32]. For these analyses we included only metastases and haemangiomas that were detected with both techniques. The sensitivity and specificity were calculated using GEE models as described above to address data clustering and grade 4 and 5 of the discrimination ratings as reader's judgment for metastasis. With combined gadoxetic acid/gadofosveset, both readers had perfect discrimination for distinguishing metastases from haemangiomas (AUC = 1); therefore, standard errors could not be computed and the resulting 95 % CIs were uninformative. Since the Obuchowski test could no longer be used to compare AUCs adjusted for clustering, we report *P* values from the standard DeLong test [33]. These same issues precluded use of the cluster-adjusted McNemar's test to compare sensitivities and specificities, so we used a standard McNemar's test.

The ratio of the signal intensity (SI) of metastases and haemangiomas to that of the adjacent liver parenchyma was calculated as SI ratio = SI_{lesion}/SI_{liver} [9]. SI ratios between metastases and haemangiomas were compared with identity Gaussian links using GEE models as described above [29].

There was no adjustment of *P* values for multiple testing. A *P* value of less than 0.05 indicated a statistically significant difference. JAFROC 4.2.1 software [34] was used to perform the AFROC analyses and MedCalc v12.7.5 (MedCalc Software, Ostend, Belgium) and R (R Core Team 2014) for other statistical computations.

Results

No immediate adverse events were reported following the combined injection of gadoxetic acid and gadofosveset trisodium in any of the 91 MRI clinical examinations included in this retrospective study. In all patients, the additional injection of gadofosveset trisodium increased the signal intensity of the vessels to a level comparable to the gadoxetic acid-enhanced liver parenchyma, thereby rendering a "plain white" liver (Fig. 2).

Detection and conspicuity of metastases

Both readers detected more metastases using combined gadoxetic acid/gadofosveset images (130 and 124 of 145, respectively) as compared to gadoxetic acid alone (104 and 103 of 145, respectively). For both readers the sensitivity was significantly higher for the combined technique (90 % and 86 %, respectively) as compared to gadoxetic acid alone (72 % and 71 %, respectively, both $P<0.01$) (Table 1).

Figure 3 demonstrates metastases in two patients that were detected by both readers on combined gadoxetic acid/gadofosveset-enhanced images but missed on gadoxetic acid alone enhanced images. Supplementary Movie 1 provides a visual impression of the actual scrolling through of a complete data set of gadoxetic acid alone as compared to combined gadoxetic acid/gadofosveset-enhanced images.

The AFROC analyses revealed significantly improved detection of metastases after injection of gadofosveset as compared to gadoxetic acid alone enhanced MRI (Fig. 4). The pooled AUC was higher for combined gadoxetic acid/gadofosveset (0.92; CI 0.88–0.96) than for gadoxetic acid alone (0.86; CI 0.83–0.89), with a statically significant difference of 0.06 (CI 0.03–0.09, $P<0.0001$). Table 1 provides a breakdown of the individual AUCs of both readers and techniques.

For both readers the PPV was lower for the combined technique (95 % and 88 %, respectively) as compared to gadoxetic acid alone (98 % and 90 %, respectively); this difference did not reach statistical significance (both $P> 0.05$) (Table 1). The false positive ratings corresponded in all cases to tiny cysts (1–2 mm).

Differentiation of metastasis and haemangioma

Figure 5 demonstrates that both metastases and haemangiomas appear hypointense on gadoxetic acid alone-enhanced images but that they show different contrast characteristics after the injection of gadofosveset trisodium. After additional injection of gadofosveset, haemangiomas show either homogenous enhancement (becoming isointense to the liver parenchyma) or a peripheral nodular enhancement (Fig. 5a, Table 2). Metastases show no or negligible enhancement in 59 % (reader 2) and 75 % (reader 1) of cases (Fig. 5b, Table 2). In the remaining cases metastases show ring, heterogeneous or central enhancement (Fig. 5c, Table 2). None of the metastases show homogenous or peripheral nodular enhancement (Table 2).

Figure 6 shows the similar SI ratios of metastases (0.38 ±0.10) and haemangiomas (0.40±0.11) on gadoxetic alone-enhanced images ($P=0.53$). Injection of gadofosveset increased the metastasis/liver SI ratio to 0.48±0.16, whereas the haemangioma/liver SI ratio was increased to 0.98 ±0.18 (almost isointense to liver tissue). This difference was statistically significant ($P < 0.001$). Note the outliers with high contrast enhancement of metastases in a patient with carcinoid tumour (same as in Fig. 5c).

The sensitivity of both readers for discrimination between metastases and haemangiomas increased significantly after injection of gadofosveset compared to gadoxetic acid alone (both $P<0.01$) (Table 3). The specificity was also increased; however, this difference did not

reach statistical significance ($P = 0.125$ and $P = 0.063$). Conventional ROC analyses revealed a statistically significant higher AUC for combined gadoxetic acid/gadofosveset as compared to gadoxetic acid alone for both readers (both $P<0.01$) (Table 3).

Discussion

Our study demonstrates that combined gadoxetic acid and gadofosveset-enhanced MRI improves detection and characterization of liver metastases compared to gadoxetic acid alone. The gadoxetic acid-enhanced liver tissue and the gadofosveset-enhanced vessels rendered the visual impression of a homogenously hyperintense “plain white” liver. This hyperintense homogenous background of the entire organ (tissues *and* vessels) improved the conspicuity of metastases, thereby significantly increasing their overall detection rate.

Most importantly, the sensitivity of lesion detection increased significantly after injection of gadofosveset. However, it should be noted that the PPV decreased slightly because the combined contrast technique led to a small number of false positives. In all cases, the false positives corresponded to tiny cysts (1–2 mm) that were simply missed on gadoxetic acid alone images and were difficult to characterize on the relatively thick (5 mm) T2-weighted images because of partial volume effects. This phenomenon demonstrates not only the importance of using all available sequences to characterize focal lesions but also the relative performance of the high spatial resolution navigator-based T1-weighted imaging methods used in the delayed phase. Until the spatial resolution of T2WI methods can be improved to match that of the T1-weighted imaging, it may be prudent to consider tiny lesions visualized on the delayed T1-weighted images as “indeterminate” since they are difficult to fully characterize on all sequences. Understanding this potential pitfall and limitations of this approach may be helpful to avoid false positive readings of tiny lesions in future studies.

We observed a rather low sensitivity (71–72 %) on gadoxetic acid alone enhanced images for detection of hepatic metastases compared to previous studies (85–95 %) [5–8]. The sensitivity for detecting hepatic metastases depends on various factors. One of the most important factors is lesion size. It is well known from past studies that the diagnostic accuracy of lesion detection using gadoxetic acid is limited for lesions 1 cm or less [7, 8]. In our study the average size of the metastases was 12 ± 11 mm and 94 of the 145 metastases (65 %) were 1 cm or less, which likely explains the lower sensitivity compared to previous studies.

The injection of gadofosveset in the hepatobiliary phase revealed different enhancement patterns of metastases and haemangiomas. Haemangiomas were homogeneously isointense to liver or demonstrated peripheral nodular enhancement that was not seen in any of the metastases. The enhancement pattern of the lesions was an important discriminatory feature that was helpful to distinguish metastases from haemangiomas.

Our study has important clinical implications. The increased sensitivity of the combined gadoxetic acid/gadofosveset-enhanced liver MRI may have a major impact on patient management and treatment. Detection of additional metastases may up-stage patients and alter the treatment strategy in individual subjects, e.g. from curative surgical resection to

chemotherapy. This also has important potential cost-effectiveness implications. Despite the increased cost of using two contrast agents, improving the accuracy of metastatic disease staging has the potential for considerable cost-savings [35].

Our study also has several limitations including its retrospective design and therefore our inability to assess the impact of this approach on patient management. Another important limitation of the combined contrast approach is that the total dose of gadolinium with two agents was higher than compared to gadoxetic acid alone. However, the combined total dose (0.1 mmol/kg) is the same as the total dose of most extracellular gadolinium-based contrast agents, which are typically administered at a dose of 0.1 mmol/kg. Therefore, we do not anticipate any increased risk of nephrogenic systemic fibrosis (NSF) related to total gadolinium exposure. A further limitation of the study is that not all metastases were histologically confirmed, which might be regarded as a drawback of our applied standard of reference. However, albeit not perfect, such an approach is frequently chosen in lesion detection studies for the reason of practicability.

In summary, combined gadoxetic acid and gadofosveset-enhanced MRI improves detection and characterization of liver metastases compared to gadoxetic acid alone. Future studies are needed to determine whether the improved diagnostic accuracy positively impacts patient management, determine which patient populations will benefit most from this approach and evaluate the overall cost-effectiveness.

Supplementary Material

Refer to Web version on PubMed Central for supplementary material.

Acknowledgments

The scientific guarantor of this publication is Scott B. Reeder. The authors of this manuscript declare no relationships with any companies whose products or services may be related to the subject matter of the article. The authors state that this work has not received any funding. Alejandro Munoz del Rio, PhD kindly provided statistical advice for this manuscript. Institutional review board approval was obtained. Written informed consent was waived by the institutional review board. Study subjects or cohorts have not been previously reported. Methodology: retrospective, cross-sectional study, performed at one institution.

References

1. Torre LA, Bray F, Siegel RL, Ferlay J, Lortet-Tieulent J, Jemal A. Global cancer statistics, 2012. CA Cancer J Clin. 2015; doi: 10.3322/caac.21262
2. Fowler KJ, Linehan DC, Menias CO. Colorectal liver metastases: state of the art imaging. Ann Surg Oncol. 2013; 20:1185–1193. [PubMed: 23115006]
3. Imam K, Bluemke DA. MR imaging in the evaluation of hepatic metastases. Magn Reson Imaging Clin N Am. 2000; 8:741–756. [PubMed: 11149677]
4. Van Beers BE, Pastor CM, Hussain HK. Primovist, Eovist: what to expect? J Hepatol. 2012; 57:421–429. [PubMed: 22504332]
5. Huppertz A, Balzer T, Blakeborough A, et al. Improved detection of focal liver lesions at MR imaging: multicenter comparison of gadoxetic acid-enhanced MR images with intraoperative findings. Radiology. 2004; 230:266–275. [PubMed: 14695400]
6. Kim HJ, Lee SS, Byun JH, et al. Incremental value of liver MR imaging in patients with potentially curable colorectal hepatic metastasis detected at CT: a prospective comparison of diffusion-

weighted imaging, gadoxetic acid-enhanced MR imaging, and a combination of both MR techniques. Radiology. 2014; :140390.doi: 10.1148/radiol.14140390

7. Motosugi U, Ichikawa T, Morisaka H, et al. Detection of pancreatic carcinoma and liver metastases with gadoxetic acid-enhanced MR imaging: comparison with contrast-enhanced multi-detector row CT. Radiology. 2011; 260:446–453. [PubMed: 21693662]
8. Muhi A, Ichikawa T, Motosugi U, et al. Diagnosis of colorectal hepatic metastases: comparison of contrast-enhanced CT, contrast-enhanced US, superparamagnetic iron oxide-enhanced MRI, and gadoxetic acid-enhanced MRI. J Magn Reson Imaging. 2011; 34:326–335. [PubMed: 21780227]
9. Motosugi U, Ichikawa T, Onohara K, et al. Distinguishing hepatic metastasis from hemangioma using gadoxetic acid-enhanced magnetic resonance imaging. Invest Radiol. 2011; 46:359–365. [PubMed: 21427594]
10. Goshima S, Kanematsu M, Watanabe H, et al. Hepatic hemangioma and metastasis: differentiation with gadoxetate disodium-enhanced 3-T MRI. AJR Am J Roentgenol. 2010; 195:941–946. [PubMed: 20858822]
11. Heiken JP. Distinguishing benign from malignant liver tumours. Cancer Imaging. 2007; 7:S1–S14. [PubMed: 17921080]
12. Ba-Ssalamah A, Uffmann M, Saini S, Bastati N, Herold C, Schima W. Clinical value of MRI liver-specific contrast agents: a tailored examination for a confident non-invasive diagnosis of focal liver lesions. Eur Radiol. 2009; 19:342–357. [PubMed: 18810454]
13. Doo KW, Lee CH, Choi JW, Lee J, Kim KA, Park CM. “Pseudo washout” sign in high-flow hepatic hemangioma on gadoxetic acid contrast-enhanced MRI mimicking hypervascular tumor. AJR Am J Roentgenol. 2009; 193:W490–W496. [PubMed: 19933623]
14. Motosugi U, Ichikawa T, Sano K, et al. Double-dose gadoxetic acid-enhanced magnetic resonance imaging in patients with chronic liver disease. Invest Radiol. 2011; 46:141–145. [PubMed: 21139506]
15. Soyer P, Dufresne AC, Somveille E, Scherrer A. Hepatic cavernous hemangioma: appearance on T2-weighted fast spin-echo MR imaging with and without fat suppression. AJR Am J Roentgenol. 1997; 168:461–465. [PubMed: 9016227]
16. Vilgrain V, Boulos L, Vullierme MP, Denys A, Terris B, Menu Y. Imaging of atypical hemangiomas of the liver with pathologic correlation. Radiographics. 2000; 20:379–397. [PubMed: 10715338]
17. Higashihara H, Murakami T, Kim T, et al. Differential diagnosis between metastatic tumors and nonsolid benign lesions of the liver using ferucarbotran-enhanced MR imaging. Eur J Radiol. 2010; 73:125–130. [PubMed: 19019608]
18. Grist TM, Korosec FR, Peters DC, et al. Steady-state and dynamic MR angiography with MS-325: initial experience in humans. Radiology. 1998; 207:539–544. [PubMed: 9577507]
19. Milot L, Haider M, Foster L, McGregor C, Law C. Gadofosveset trisodium in the investigation of focal liver lesions in noncirrhotic liver: Early experience. J Magn Reson Imaging. 2012; 36:738–742. [PubMed: 22488745]
20. Bannas P, Motosugi U, Hernando D, Rahimi MS, Holmes JH, Reeder SB. Combined gadoxetic acid and gadofosveset enhanced liver MRI: a feasibility and parameter optimization study. Magn Reson Med. 2015; doi: 10.1002/mrm.25554
21. Itai Y, Furui S, Araki T, Yashiro N, Tasaka A. Computed tomography of cavernous hemangioma of the liver. Radiology. 1980; 137:149–155. [PubMed: 7422836]
22. Caseiro-Alves F, Brito J, Araujo AE, et al. Liver haemangioma: common and uncommon findings and how to improve the differential diagnosis. Eur Radiol. 2007; 17:1544–1554. [PubMed: 17260159]
23. Horton KM, Bluemke DA, Hruban RH, Soyer P, Fishman EK. CT and MR imaging of benign hepatic and biliary tumors. Radiographics. 1999; 19:431–451. [PubMed: 10194789]
24. Nagle SK, Busse RF, Brau AC, et al. High resolution navigated three-dimensional T(1)-weighted hepatobiliary MRI using gadoxetic acid optimized for 1.5 Tesla. J Magn Reson Imaging. 2012; 36:890–899. [PubMed: 22648633]

25. Kuhn JP, Holmes JH, Brau AC, Iwadate Y, Hernando D, Reeder SB. Navigator flip angle optimization for free-breathing T1-weighted hepatobiliary phase imaging with gadoxetic acid. J Magn Reson Imaging. 2014; 40:1129–1136. [PubMed: 24214890]

26. Ward J, Naik KS, Guthrie JA, Wilson D, Robinson PJ. Hepatic lesion detection: comparison of MR imaging after the administration of superparamagnetic iron oxide with dual-phase CT by using alternative-free response receiver operating characteristic analysis. Radiology. 1999; 210:459–466. [PubMed: 10207430]

27. Chakraborty DP, Berbaum KS. Observer studies involving detection and localization: modeling, analysis, and validation. Med Phys. 2004; 31:2313–2330. [PubMed: 15377098]

28. Chakraborty DP, Winter LH. Free-response methodology: alternate analysis and a new observer-performance experiment. Radiology. 1990; 174:873–881. [PubMed: 2305073]

29. Liang KY, Zeger SL. Longitudinal data analysis using generalized linear models. Biometrika. 1986; 73:13–22.

30. Obuchowski NA. On the comparison of correlated proportions for clustered data. Stat Med. 1998; 17:1495–1507. [PubMed: 9695194]

31. Jung SH, Kang SH, Ahn C. Chi-square test for R × C contingency tables with clustered data. J Biopharm Stat. 2003; 13:241–251. [PubMed: 12729392]

32. Obuchowski NA. Nonparametric analysis of clustered ROC curve data. Biometrics. 1997; 53:567–578. [PubMed: 9192452]

33. DeLong ER, DeLong DM, Clarke-Pearson DL. Comparing the areas under two or more correlated receiver operating characteristic curves: a nonparametric approach. Biometrics. 1988; 44:837–845. [PubMed: 3203132]

34. JAFROC Software v 4.2.1. Available via http://www.devchakraborty.com

35. Zech CJ, Korpraphong P, Huppertz A, et al. Randomized multicentre trial of gadoxetic acid-enhanced MRI versus conventional MRI or CT in the staging of colorectal cancer liver metastases. Br J Surg. 2014; 101:613–621. [PubMed: 24652690]

Key Points

- Combined gadoxetic acid and gadofosveset-enhanced liver MRI significantly improves detection of metastases.
- The combined enhancement technique improves the accuracy to differentiate metastases from haemangiomas.
- Prospective studies need to determine the clinical impact of the combined technique

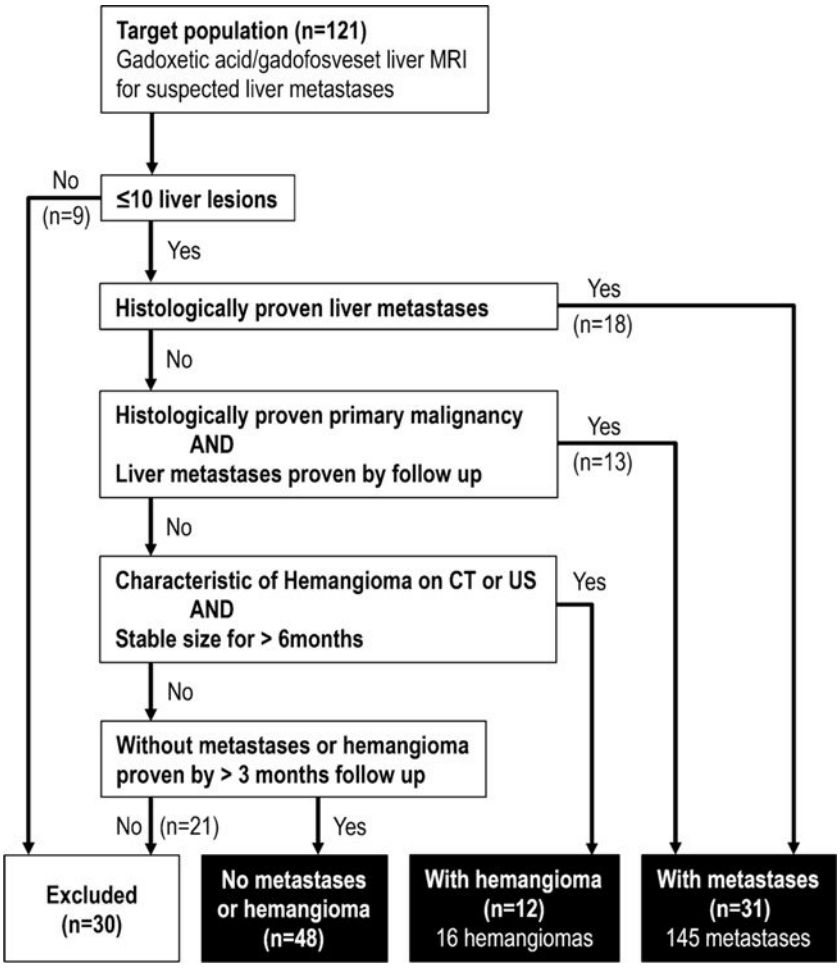

Fig. 1.

Inclusion criteria flow chart. Patients that underwent both gadoxetic acid alone and combined gadoxetic acid/gadofosveset-enhanced liver MRI were included in this study for the evaluation of liver lesion detection and characterization. *CT* computed tomography, *US* ultrasound

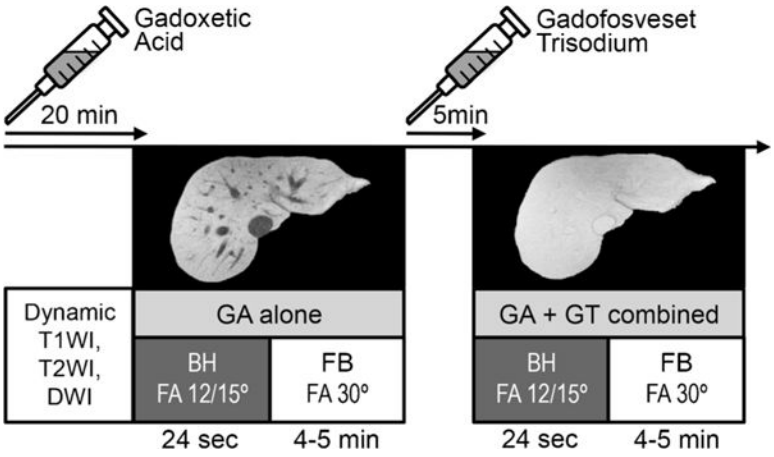

Fig. 2.

Overview of the clinical protocol. Twenty minutes after injection of gadoxetic acid, breathheld (*BH*) and respiratory-gated free-breathing (*FB*) T1-weighted imaging was performed at 12° (1.5 T) or 15° (3 T) and 30° (both 1.5 and 3 T) flip angle, respectively. Five minutes after injection of gadofosveset trisodium, imaging was repeated with identical imaging parameters during the steady-state blood pool phase of gadofosveset while still in the hepatobiliary phase of gadoxetic acid. *T1WI* T1-weighted imaging, *T2WI* T2-weighted imaging, *DWI* diffusion-weighted imaging, *GA* gadoxetic acid, *GT* gadofosveset trisodium, *FA* flip angle. Note the isointensity of the vessels relative to the liver tissue after injection of gadofosveset

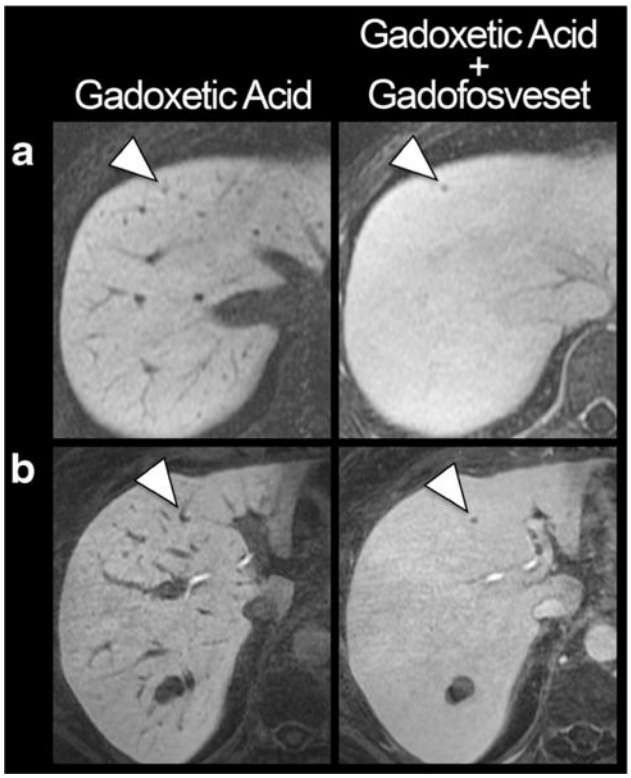

Fig. 3.

Improved conspicuity of small liver metastases. T1-weighted images with gadoxetic acid alone and in combination with gadofosveset in a 41-year-old woman with melanoma **(a)** and a 53-year-old woman with oesophageal cancer **(b).** Note the improved conspicuity of the metastases (*arrowheads*), particularly of the perivascular lesion in **b.** Both histologically confirmed metastases were missed by both readers on gadoxetic alone enhanced images but detected on combined gadoxetic acid/gadofosveset-enhanced images. The two patients had only one and two other metastases, respectively

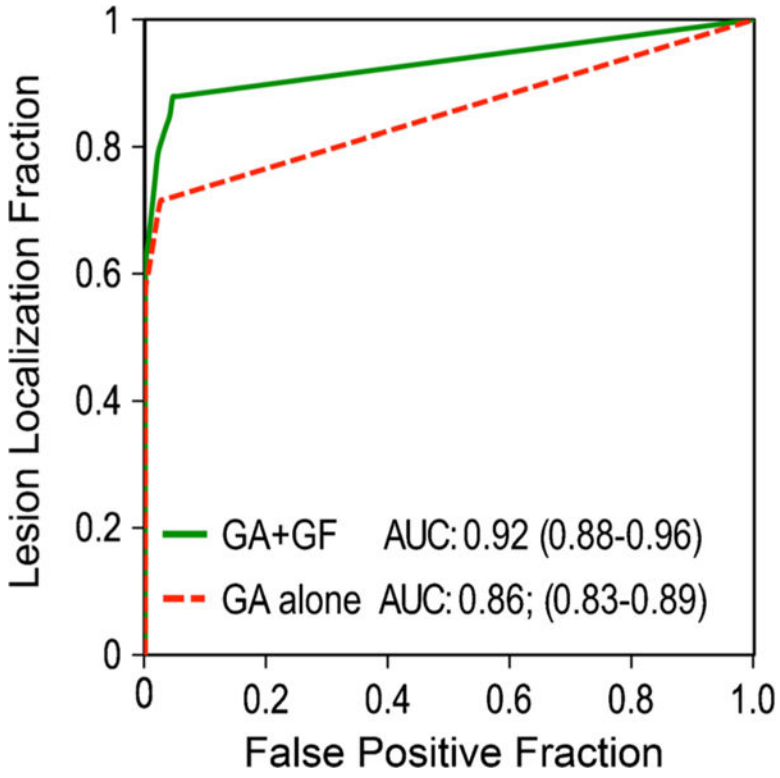

Fig. 4.

AFROC analyses of gadoxetic acid alone vs. combined gadoxetic acid and gadofosveset-enhanced MRI for detection of liver metastases. Reader-averaged areas under the curve (AUC) of alternative free-response ROC (AFROC) analyses of gadoxetic acid (GA) and combined gadoxetic acid/gadofosveset (GA + GF)-enhanced MRI serve as the figure of merit. The AUC is significantly higher for combined gadoxetic acid/gadofosveset (0.92) than for gadoxetic acid alone (0.86), with a mean difference of 0.06 (CI 0.03–0.09, $P < 0.0001$)

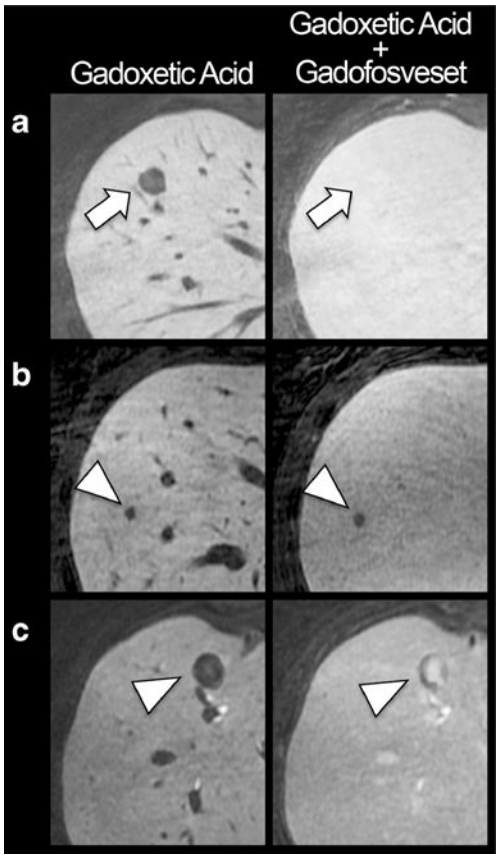

Fig. 5.

Different enhancement patterns of haemangiomas and metastases. All lesions appear hypointense compared the liver tissue on gadoxetic acid alone enhanced liver MRI. **a** Example of a 50-year-old woman with haemangioma (*arrow*). The additional injection of gadofosveset in the hepatobiliary phase of gadoxetic acid renders the haemangioma isointense to liver tissue. **b** Example of a 58-year-old woman with a metastases of colorectal cancer, showing no or negligible enhancement after injection of gadofosveset (*arrowhead*). **c** Example of a 51-year-old man with metastases of a neuroendocrine carcinoid tumour, showing central enhancement after injection of gadofosveset (*arrowhead*)

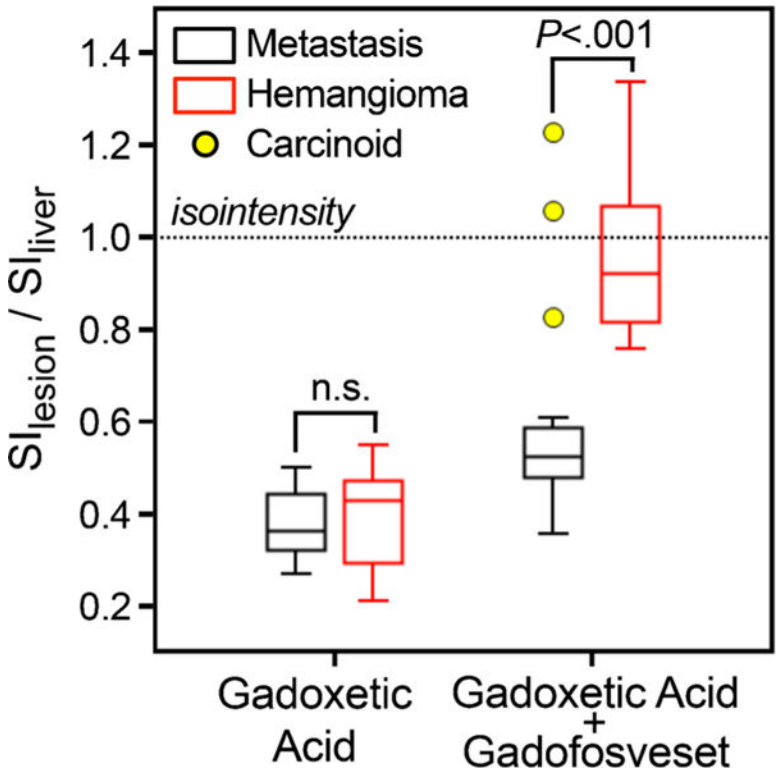

Fig. 6.

Improved differentiation of metastases vs. haemangiomas with combined gadoxetic acid and gadofosveset-enhanced liver MRI. Using gadoxetic acid alone does not allow differentiation of metastases from haemangiomas by signal intensity ($P = 0.51$); both appear hypointense and have low SI ratios relative to the liver. Injection of gadofosveset leads only to a slight increase of the liver/metastasis SI ratio, whereas the haemangioma/liver SI ratio is dramatically increased, thereby rendering the SI ratios of haemangiomas and metastases significantly different ($P<0.001$). *Dotted horizontal line* indicates isointensity of lesions with liver tissue. Outliers (*yellow circles*) represent contrast-enhancing metastases in a patient with carcinoid tumour. Note, however, that the enhancement pattern (central) of these carcinoid metastases made it easy to distinguish all of these lesions from haemangiomas (see Fig. 5)

Table 1

Sensitivity, positive predictive value and AFROC-AUC for detection of hepatic metastases

Reader	Technique	Sensitivity			PPV			AFROC-AUC	
1	Gadoxetic acid	104/145	72 %	(62–84 %)	104/106	98 %	(95–100 %)	0.86	(0.79–0.92)
	Gadoxetic acid + gadofosveset	130/145	90 %	(83–97 %)	130/137	95 %	(91–99 %)	0.92	(0.87–0.97)
	P value	***P*=0.0038**			*P* = 0.051			***P*=0.0020**	
2	Gadoxetic acid	103/145	71 %	(61–82 %)	103/114	90 %	(79–100 %)	0.87	(0.81–0.93)
	Gadoxetic acid + gadofosveset	124/145	86 %	(78–94 %)	124/141	88 %	(77–100 %)	0.93	(0.88–0.97)
	P value	***P*=0.0038**			*P*=0.071			***P* =0.0017**	

Numbers indicate lesions that were used for calculating the percentages with 95 % confidence intervals (in parenthesis). Sensitivities and specificities are calculated using each marked lesion as readers' judgment for a positive finding. *P* values < 0.05 indicate statistical significant differences, significant values are in bold

PPV positive predictive value, *AFROC* alternative free-response receiver-operating characteristic, *AUC* area under the curve

Table 2

Enhancement pattern of metastases and haemangiomas on gadoxetic acid vs. gadoxetic acid/gadofosveset-enhanced liver MRI

	Reader 1								Reader 2							
	Gadoxetic acid alone				Gadoxetic acid/gadofosveset				Gadoxetic acid alone				Gadoxetic acid/gadofosveset			
Enhancement pattern	Metastasis		Haemangioma		Metastasis		Haemangioma		Metastasis		Haemangioma		Metastasis		Haemangioma	
None/negligible	92	88 %	15	94 %	78	75 %	0	0 %	72	70 %	15	94 %	61	59 %	0	0 %
Central	2	2 %	0	0 %	6	6 %	0	0 %	15	14 %	0	0 %	9	9 %	0	0 %
Ring	8	8 %	0	0 %	12	11 %	0	0 %	8	8 %	0	0 %	13	13 %	0	0 %
Heterogeneous	2	2 %	1	6 %	8	8 %	0	0 %	8	8 %	1	6 %	20	19 %	0	0 %
Peripheral nodular	0	0 %	0	0 %	0	0 %	5	31 %	0	0 %	0	0 %	0	0 %	2	13 %
Homogenous	0	0 %	0	0 %	0	0 %	11	69 %	0	0 %	0	0 %	0	0 %	14	87 %
Total	104	100 %	16	100 %	104	100 %	16	100 %	103	100 %	16	100 %	103	100 %	16	100 %

Total numbers correspond to the number of lesions that each reader detected on gadoxetic acid alone enhanced images. Percentages are rounded

Table 3

Conventional ROC analysis to distinguish metastasis from haemangioma

Reader	Technique	Sensitivity			Specificity			ROC-AUC	
1	Gadoxetic acid	89/104	86 %	(77–94 %)	12/16	75 %	(45–100 %)	0.87	(0.72–1.00)
	Gadoxetic acid + gadofosveset	102/104	98 %	(95–100 %)	16/16	100 %	(79–100 %)*	1.00	(1.00–1.00)
	P value	***P*=0.0002***			*P* = 0.125*			***P*=0.0084***	
2	Gadoxetic acid	94/103	91 %	(84–98 %)	11/16	69 %	(40–100 %)	0.92	(0.87–0.97)
	Gadoxetic acid + gadofosveset	102/103	99 %	(97–100 %)	16/16	100 %	(79–100 %)*	1.00	(1.00–1.00)
	P value	***P*=0.0078***			*P*=0.063*			***P*=0.0084***	

Numbers indicate lesions that were used for calculating the percentages with 95 % confidence intervals (in parenthesis). Sensitivities and specificities are calculated using confidence ratings 0–2 vs 3–4 as the cut-off. Asterisks indicate 95 % confidence intervals or *P* values that are unadjusted for clusters because GEE models did not attain convergence. *P* values < 0.05, shown in bold, indicate statistically significant differences

ROC receiver-operating characteristic, *AUC* area under the curve